DOI: 10.5604/01.3001.0053.6699

Volume 117 • Issue 2 • April 2023

Journal of Achievements in Materials and Manufacturing Engineering

International Scientific Journal published monthly by the World Academy of Materials and Manufacturing Engineering

The characterization study of inhibited silica/silicate scale using vinyl sulfonated copolymer (VS-Co)

R.A.b. Sazali [a,*], K.S. Sorbie [b,c], L.S. Boak [b,c], A.Z. Azman [a], I.b. Mohd Saaid [d,e], A.b. Dollah [a], N.Z.b. Kassim Shaari [a], K.N.b. Ismail [a]

[a] School of Chemical Engineering, College of Engineering, Universiti Teknologi MARA, Shah Alam, 40450, Selangor, Malaysia

[b] Flow Assurance and Scale Team, Institute of GeoEnergy Engineering, Heriot-Watt University, UK EH14 4AS, Edinburgh, Scotland, United Kingdom

[c] School of Energy, Geoscience, Infrastructure and Society (EGIS), Heriot-Watt University, UK EH14 4AS, Edinburgh, Scotland, United Kingdom

[d] Centre of Research in Enhanced Oil Recovery (COREOR), Universiti Teknologi PETRONAS, 32610 Seri Iskandar, Perak, Malaysia

[e] Petroleum Engineering Department, Faculty of Engineering, Universiti Teknologi PETRONAS, 32610 Seri Iskandar, Perak, Malaysia

* Corresponding e-mail address: rozana592@uitm.edu.my

ORCID identifier: https://orcid.org/0000-0002-7224-5088 (R.A.b.S.)

ABSTRACT

Purpose: Silica/silicate scale is a significant problem, especially in oilfield production during Alkaline Surfactant Polymer (ASP) flooding, where chemical inhibitors are the preferred method to prevent them. In this study, the effect of inhibitor vinyl sulfonated copolymer (VS-Co) on silica/silicate scale formation was analysed using X-Ray Diffraction (XRD) and Fourier-transform infrared spectroscopy (FTIR).

Design/methodology/approach: The functional group type of VS-Co are sulfonate ions, SO^{3-}, and these interact in the scaling process. Bulk-inhibited scaling brine tests were conducted at 60°C and pH 8.5. During these tests, the silicon brine (with VS-Co) representing the inhibited ASP leachate was mixed with a magnesium brine representing the connate water to replicate reservoir conditions during ASP flooding. The samples tested in this study were non-inhibited Si/Mg mixed brine of 60 ppm Mg^{2+} and 940 ppm Si^{4+} (60Mg:940Si) as a blank, and inhibited 60Mg:940Si mixture with various VS-Co concentrations of 20 ppm, 50 ppm, and 100 ppm. The inhibition efficiency of the VS-Co was determined, followed by the characterisation study of the silica/silicate scale deposited from both test conditions.

Findings: The IR spectra of all 60Mg:940Si samples show a similar peak at 1050 cm^{-1} to 1080 cm^{-1}, attributed to a Si-O covalent bond and a band at 790 cm^{-1} to 800 cm^{-1} showing the presence of Si-O-Si stretching. XRD patterns produced a broad scattering peak for all samples at 2θ of 24° showing that the samples are amorphous silica. For tests of high Mg^{2+} in the brine mix, 900Mg:940Si, a mix of crystalline silica and crystalline magnesium silicate was produced. Based on these results, it can be concluded that the scale formed even with 100 ppm of VS-Co present. Further studies are required to address how to mitigate scale formation effectively in the future.

Research limitations/implications: Based on the research conducted, we can conclude that the VS-Co alone could not significantly inhibit the formation of silica/silicate scale even at the highest concentration (100 ppm) of VS-Co. However, having VS-Co present caused an alteration in IR spectra frequency which requires further investigation to assess how best to develop the inhibiting properties of the VS-Co product. The application of nanoparticles and their successful stories spark the interest of authors in searching for an efficient method of managing the silica/silicate scale where the modification of potential scale inhibitor (SI) with nanoparticles may be able to improve the inhibition efficiency towards the silicate/silicate scale.

Practical implications: The presence of VS-Co in the scaling brine only slightly inhibits the Mg^{2+} ion (initially comes from connate water) from reacting. It is worth further investigation on how this VS-Co can make it happen. Hence, the functional groups responsible for this may be altered by adding other functional groups to provide a synergistic effect in preventing this silica/silicate scale; or by modifying the VS-Co with nanoparticles to improve their adsorption/desorption capacity.

Originality/value: The newly developed technique in analysing the inhibition mechanism of a chemical inhibitor using various spectroscopic analysis is promising where an alteration in the spectra may provide proof of the chemical's inhibition efficiency.

Keywords: Silica/Silicate scale, Alkaline surfactant polymer (ASP) flooding, Vinyl sulfonated copolymer (VS-Co), X-ray diffraction (XRD), Fourier-transform infrared spectroscopy (FTIR)

Reference to this paper should be given in the following way:

R.A.b. Sazali, K.S. Sorbie, L.S. Boak, A.Z. Azman, I.b. Mohd Saaid, A.b. Dollah, N.Z.b. Kassim Shaari, K.N.b. Ismail, The characterization study of inhibited silica/silicate scale using vinyl sulfonated copolymer (VS-Co), Journal of Achievements in Materials and Manufacturing Engineering 117/2 (2023) 57-70. DOI: https://doi.org/10.5604/01.3001.0053.6699

PROPERTIES

1. Introduction

Silica and silicate scale formation have been encountered in various operation plants/systems such as steam generators, desalination, water treatment, geothermal, and oilfield production [1-5]. According to Wang and Wei (2016), silica/silicate scale formation occurs through silica condensation and polymerisation mechanisms [6]. The formation of silica/silicate scale is usually controlled by a few factors such as amorphous silica solubility, temperature, composition, solution pH, rate of growth, system dimension, hydrodynamic conditions of brine flow, and concentration of colloidal particles [1,7].

In the oil and gas industry, alkaline surfactant polymer (ASP) is a relatively new and still evolving enhanced oil recovery (EOR) technique. When using ASP flooding in sandstone reservoirs, silica/silicate scaling is almost unavoidable in the production well [8]. This phenomenon can lead to various technical problems, such as pipe and equipment obstruction, which eventually cause damage, reduced production, and economic losses. Many studies have been conducted to prevent the scaling or at least to slow down the silica/silicate scale formation to prolong the lifespan of existing assets and infrastructure [2, 9-11]. The expenditure to eradicate this problem was estimated at 0.8 billion USD in Great Britain, 3 billion USD in Japan, and 9 billion USD in the USA]. Hence, engineers must understand the mechanisms of silica/silicate scale formation, its type, and how to prevent or slow down the scaling process.

Numerous studies [3,8, 13-16] have described the formation of silica/silicate scale as a complex process arising as a consequence of silica dissolution, polymerisation, and precipitation with other multivalent ions. Three important factors affect the silica formation rate and quantity; pH, ion concentration, and temperature [4,7]. Silica is not only dissolved in water but solubilised through hydrolysis reactions to form dissolved silica called silicic acid at a pH of 7, represented in reaction (1):

$$SiO_2 + 2H_2O \leftrightarrow H_4SiO_4 \quad \text{(Reaction 1)}$$

At pH > 7 or alkali conditions, the silicic acid (H_4SiO_4) becomes ionised; hence reducing the concentration of H_4SiO_4, causing the system to re-equilibrate by dissolving additional SiO_2 into solution [3]. Fatah (2021) reported that silica dissolution is a critical factor that leads to the supersaturation condition in the production system. This supersaturation condition has induced the silica/silicate scale formation, which affects not only the production wells but may lead to severe formation damage [17]. When the pH is high, the quartz in the formation is dissolved by the solution, resulting in dissolved monomeric silica as shown in reaction (2):

$$SiO_4 + NaOH \rightarrow Si(OH)_3O\text{-}Na^+ \quad \text{(Reaction 2)}$$

There is often neutral (pH7) connate water near or in the wellbore. When the high pH of the alkaline surfactant polymer propagates into the production well, both of these solutions will comingle hence neutralising the high pH alkaline water. When the pH decreases, this results in the polymerisation of dissolved silica to form colloidal silica nanoparticles [18]. It is well known that the magnesium silicate system is highly pH-dependent. When pH < 7, magnesium silicate scale precipitation does not occur, as silica is only available in the unionised form. However, when the pH is increased, it is very likely for magnesium silicate to form with the general chemical structure shown in Figure 1.

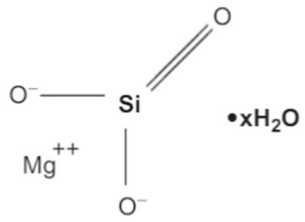

Fig. 1. A schematic of the structure of magnesium silicate [19]

Silica/Silicate scale is very difficult to remove chemically once formed. The only method being used traditionally is mechanical removal. A diverse range of polymers and chemicals have been developed and tested as scale inhibitors (SIs) for preventing or retarding the formation of amorphous silica and magnesium silicate scales [20]. It is learned that the biopolymers have interesting qualities such as their lightness, strong mechanical properties, and appealing functionality, plus their insensitivity toward brine salinity, but somehow present enormous potential for environmental application because of their biodegradability, chemical adaptability, reactivity, biocompatibility, and nontoxicity; though this is still under laboratory investigation [21].

A couple of studies have tested various SI formulations from different manufacturers by reproducing the field condition using synthetic brine solutions. The performance of these various SI tested, i.e., in inhibiting the silica/silicate scale, has been compared to a brine acidification technique that is normally used for geothermal field operations in Mak-Ban field, Philippines. They concluded that brine acidification was more effective than the tested Sis, but this tends to increase the corrosion rate of steel significantly [6, 22-23]. Increasing the pH value to 10.5 and the Ca/Si ratio > 1.25 mitigated silica/silicate scaling effectively by forming calcium-silicate-hydrate phases [24].

The promising application of nanoparticles in various industrial applications is worth further study by synthesising and characterising various types of nanoparticles to be embedded with the commercial SI [25-28]. Nanobubbles may not represent perfect inhibition effectiveness for corrosion and scaling of calcium carbonate and silica on the steel surface, where it can only mitigate up to 50% [29]. A new approach has been developed to study the performance of silica/silicate scale inhibitor chemistries by a Kinetic Turbidity Test (KTT) method and static bottle test method under field application conditions [30,31].

The scale management method that is most used to control downhole scale formation is called a 'squeeze treatment'. This treatment is performed near the wellbore by injecting a chemical inhibitor [32]. A squeeze treatment is where the chemical inhibitor is injected or 'squeezed' into the rock formation. When the good returns to production, the chemical will slowly return through a desorption or redissolution process into the produced fluid, where the inhibitor concentration remains greater than the required level to prevent scale deposition. This is called the Minimum Inhibitor Concentration or MIC. A 'squeeze lifetime' is when the inhibitor concentration in the produced fluid exceeds the MIC.

Laboratory testing data for SI selection on both silica/silicate and other scales by [5] suggested that the MIC of Product C (a combination of phosphonate inhibitor + unknown silicate inhibitor) is 25 ppm, though there was no information available on this unknown silicate inhibitor plus there will be cost incurred due to the requirement of adding the phosphonate. In addition, it was reported that flocculation was observed at dosages higher than MIC due to trapping within the colloidal silica matrix; hence determining the accurate MIC is crucial. Non-ionic polymers, i.e., poly(2-ethyl-2-oxazoline) PEOX, poly(vinyl pyrrolidone) PVP, polyethylene polypropylene block copolymer, PL68, were tested at 50 ppm in 650 mg/L silica as SiO_2 solution, pH 7.0, 40 °C showing IE % between 40 to 70 % [34-35]. Whereas a nonpolymeric additive, i.e. propylene glycol PGL shows poor performance of < 10% IE and can be ranked as PEOX > PL68 > PVP >> PGL. Research by [36] learned that the synergistic effect of antiscalants (A: acrylic homopolymer, B: carboxylic sulfone copolymer, C: carboxylic sulfone non-ionic terpolymer) and the antiscalant composition (10 different mixtures) at 6.5 ppm minimised the cleaning needs of the silicate-stibnite deposits in reinjection wells of geothermal power plants located in the west coast of Turkey.

As silica/silicate scale is covalently bonded and amorphous in nature, conventional SI cannot inhibit them through either a nucleation or crystal growth inhibition

mechanism [37]. However, if the silica/silicate scale can be dispersed, it will prolong the time prior to the silica/silicate scale being formed. One study [38] noted that a good dispersant would be a polymer species with M.Wt. < 10,000 Da with carboxylic acid and sulfonic acid groups. Following the evidence suggested [38], VS-Co with the schematic structure shown in Figure 2 has been tested in this work as a potential silica/silicate SI/dispersant. In addition to that, VS-Co is used in several North Sea fields, which display good scale inhibition properties for both barium sulphate and calcium carbonate scales [39].

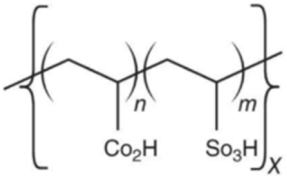

Fig. 2. Structure of vinyl sulfonated copolymer (VS-Co) [33]

Due to the fact that conventional SI may not be efficient in totally inhibiting this silica/silicate scale, it is worth testing VS-Co as the potential SI where it is postulated that the VS-Co may be able to disperse the nucleus of the silica/silicate scale i.e. the monomeric silicate anions, or dimers so that they are not polymerising further to produce amorphous silica/silicate scale. To prove this, the efficiency of the VS-Co to inhibit this silica/silicate scale is being investigated by studying the precipitates produced in both blank non-inhibited and VS-Co-inhibited mixed brine. This can be done by determining the IE % of the VS-Co (analysing by using Inductively coupled plasma-optical emission spectrometry, ICP-OES) and characterising the precipitates using XRD and FTIR.

2. Experimental details

The laboratory procedures are divided into three parts; which are i) the static bottle test, ii) the static inhibition efficiency (IE) test, and iii) the characterisation study. In the static bottle test, the Si/Mg mixed brine (blank solution known as non-inhibited scaling brine) was reproduced in the laboratory to replicate the reservoir formation under ASP flooding. In another set of experiments (Static IE Test), the VS-Co was added to the scaling brine as an inhibition strategy of the silica/silicate scaling. This will be denoted as the inhibited scaling brine. The last procedure was characterising the silica/silicate deposit formed in the blank solution and the inhibited brine using XRD and FTIR.

2.1. Materials and sample preparation

Brine preparation: 1800 ppm and 120 ppm magnesium brine (MB) were prepared by dissolving 75.3 gram and 5.02 gram of magnesium chloride hexahydrate ($MgCl_2.6H_2O$) salt in individual 5 L of distilled water, respectively. 1880 ppm of silicon brine (SB) was prepared by dissolving 71 grams of sodium metasilicate pentahydrate ($Na_2SiO_3.5H_2O$) salt in another 5 L of distilled water. It is worth noting that the low-Mg condition was tested for the blank solution and the VS-Co IE Test. Note that this high-Mg brine is only being used in precipitates characterisation (without the presence of VS-Co).

Scale Inhibitor Solution Preparation: 10,000 ppm active SI stock (of the VS-Co) was prepared before being further diluted in 250ml SB to obtain various active SI concentrations (i.e. 20 ppm, 50 ppm, and 100 ppm) in the final mixed brine by mixing SB with MB in 50:50 ratios. Hence, the initial SI concentrations prepared to need to be higher by a factor of 2 to account for the mix ratio. A non-inhibited blank SB brine was measured out to represent a blank solution.

Quench Solution Preparation: 50 grams of sodium hydroxide (NaOH) and 50 grams of disodium ethylenediaminetetraacetic acid (EDTA) were dissolved in 5L distilled water to prepare a 1% EDTA/NaOH solution.

2.2. Static bottle test and static inhibition efficiency bottle test

The procedure in this work was adapted from previous work [10-11, 40]. The mixture of brine concentration 60Mg: 940Si at test conditions of 60°C and pH8.5 was chosen as the blank base case (i.e., non-inhibited sample) to study the efficiency of the VS-Co as a scale inhibitor. The samples were allowed to react at a pH of 8.5 which is believed will promote most of the magnesium silicate to form. A reaction at a pH less than 8 will not induce the ionisation of the monomeric silica, whereas reacting at a pH of more than 9 will aggravate the magnesium hydroxide $Mg(OH)_2$ scale formation. The samples were heated to 60°C to replicate the field condition. Various mixed VS-Co concentrations, i.e. 20 ppm, 50 ppm, and 100 ppm, were added to the 60Mg:940Si to replicate the VS-Co inhibited mixed brines of 60Mg:940Si:20VS-Co, 60Mg:940Si:50VS-Co, and 60Mg:940Si:100VS-Co respectively. After mixing, the solutions were all adjusted to pH 8.5. The solutions were then ICP-sampled at 2 and 22 hours at the tested temperature and pH. 1 ml of supernatant was sampled and quenched in 9 ml of 1% EDTA/NaOH solution before being analysed by ICP-OES.

All solutions were prepared in duplicate. To ensure its repeatability and reproducibility, the results for the duplicates must be less than 5% in differences. After 22 hours, one set of test bottles was filtered using 0.2 µm filter paper. The precipitates collected were allowed to dry in a desiccator for at least 24 hours.

The other set of 22-hour duplicate samples of the blank and inhibited mixed brines were physically observed and photographed over a five days duration prior to being filtered, as above. The precipitates collected were then analysed using various spectroscopic techniques such as ESEM/EDAX, FTIR, and XRD to determine the type and morphology of the scale produced. The spectra generated were analysed and compared with three (3) commercial samples; magnesium silicate ($MgO.SiO_2$), magnesium hydroxide ($Mg(OH)_2$), and amorphous silica (SiO_2). The methodology adopted in this experiment is simplified and summarised in Figures 3 and 4.

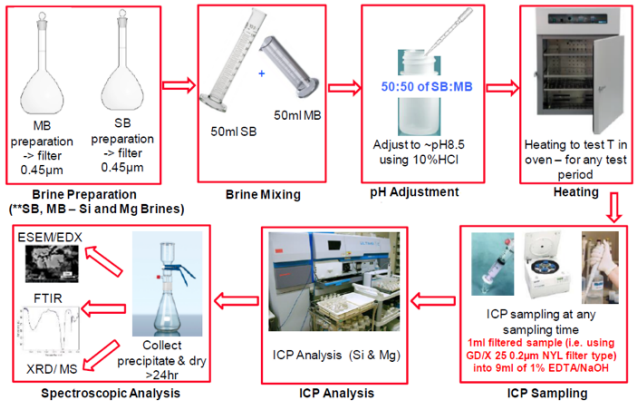

Fig. 3. Silica/silicate scale static bottle test experimental methodology – blank/ non-inhibited samples [11]

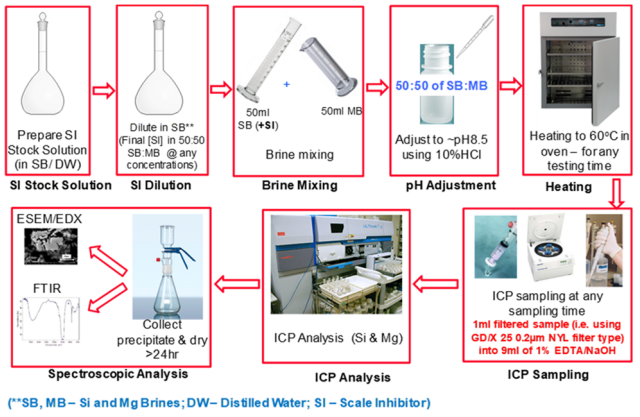

Fig. 4. Silica/silicate scale inhibition efficiency (IE) test experimental methodology – VS-Co inhibited samples [11]

2.3. VS-Co inhibition efficiency calculations

Inhibition efficiency is calculated by modifying the static method used for barium sulphate. However, since we are producing magnesium silicate scales, the measurements and calculations need to be performed for both the Mg and the Si ions, as explained below. The inhibition efficiency of any SI (IE %) to inhibit the silica/silicate scaling is calculated using Equation (1) [41]:

$$IE\ \%(t) = \frac{(M_B - M_I)x100}{M_B} = \frac{(C_O - C_B) - (C_O - C_I)x100}{(C_O - C_B)} = \frac{(C_I - C_B)x100}{(C_O - C_B)} \quad (1)$$

where:

M_B – mass of silicon (or other cations) precipitated in supersaturated blank solution, mg;

M_I – mass of silicon (or other cations) precipitated in a test solution, mg;

C_O – concentration of silicon (or other cations) originally in solution (i.e. t=0), ppm

C_I – concentration of silicon (or other cations) at sampling, ppm;

C_B – concentration of silicon (or other cations) in the blank solution (no inhibitor) at the same conditions and sampling time as C_I above, ppm;

(t) – sampling time, hour.

The IE Mg % is the inhibition efficiency percentage calculated using magnesium (Mg) as the scaling ion, i.e. the percentage of magnesium ion that can be prevented from precipitating in the inhibitor-containing brine as compared to the amount of magnesium ion precipitated in the blank solution. The IE Mg % value here is interpreted as the inhibition efficiency percentage of the tested inhibitor towards amorphous magnesium silicate scale formation.

The IE Si % is the inhibition efficiency percentage calculated using silicon (Si) as the scaling ion, i.e. the percentage of silicon ion that can be prevented from precipitating in the inhibitor-containing brine as compared to the amount of silicon ion precipitated in the blank solution. The IE Si % value here is interpreted as the inhibition efficiency percentage of the tested inhibitor towards amorphous silica scale formation.

2.4. X-ray diffraction (XRD)

The X-ray diffractometer patterns were obtained using a PANalytical's X'Pert PRO setup at room temperature using Cu K-alpha sources with a wavelength of 1.540598 Å. Four (4) 60Mg:940Si samples with different concentrations of VS-Co inhibitor were analysed at operating conditions of 45 kV and 20 mA with a continuous scanning range of 2θ =10 – 90 ° for 3 minutes per sample.

2.5. Fourier transform infrared (FTIR)

The FTIR spectra of the samples were obtained using a Spectrum 100 spectrometer (PerkinElmer, USA) which was equipped with a mercury-cadmium-telluride (MCT) detector in the wavelength range from 650 to 4000 cm^{-1} alongside a universal attenuated total reflectance accessory (ATR) with a diamond prism. The FTIR spectra of all samples were recorded on a Perkin Elmer Paragon 1000PC FTIR spectrometer using a diamond crystal. The spectra were measured in the wavenumber range 450-4400 cm^{-1}.

3. Results and discussion

3.1. Physical observation

All samples were physically observed, photographed, and/or ICP-sampled. The photos of the scaled brine are shown in Figure 5. It is postulated that a significant amount of inhibitor should slow down or prevent scale formation.

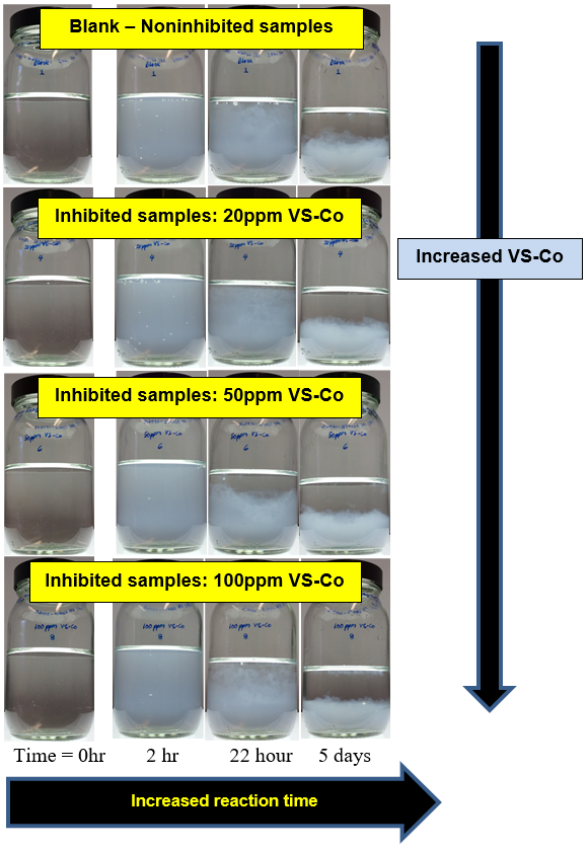

Fig. 5. Physical observation of the precipitate produced in a non-inhibited (blank) and VS-Co inhibited 60Mg:940Si system

However, no obvious differences (in terms of the cloudiness) can be observed from the photographs for the various VS-Co concentrations in the mixed Si/Mg scaling solution. The ICP-OES analysis results, however, highlight the differences in the supernatant of the blank and inhibited mixed brines after being sampled at 2 and 22 hours, respectively.

3.2. VS-Co inhibition efficiency

Figure 6 shows the percentage of scaling ions, i.e. Mg^{2+} and Si^{4+}, reacted after 2 and 22 hours, respectively. It can be noted that the presence of VS-Co in the scaling brine only slightly inhibits the Mg^{2+} ion from reacting. However, almost no difference in terms of the percentage amount of Si^{4+} ions that reacted in the blank and the VS-Co inhibited scaling solution is observed.

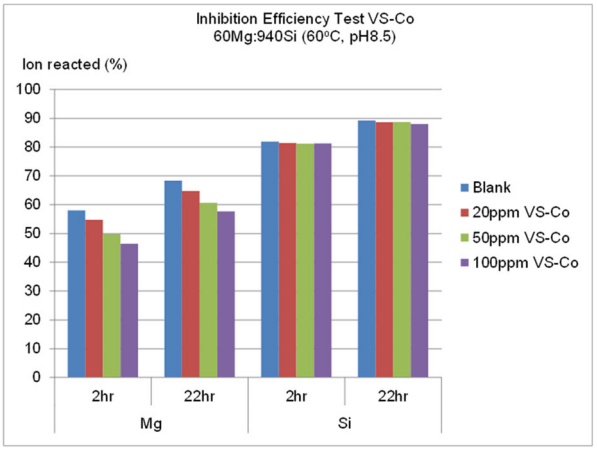

Fig. 6. % of ions reacted in non-inhibited (Blank), and VS-Co inhibited 60Mg:940Si system

Figure 7 shows the IE % calculated from Equation (1) using the Mg^{2+} and Si^{4+} ion as the scaling ion, Co, respectively. Hence, it can be stated that VS-Co only slightly inhibited the Mg^{2+} ion, and it follows the trend of a higher VS-Co concentration giving a higher IE_{Mg} %.

However, VS-Co failed to stop the Si^{4+} from further polymerising even with 100 ppm of VS-Co present. This is denoted by the IE_{Si} % being zero for all VS-Co concentrations.

3.3. Crystallographic structure of precipitates using XRD

Magnesium silicate scales were analysed using XRD and FTIR. The precipitate produced from the various test samples, i.e. 60Mg:940Si with/without different amounts of VS-Co of 20 ppm, 50 ppm,100 ppm, and a blank sample of non-inhibited 900Mg:940Si was analysed using XRD and FTIR.

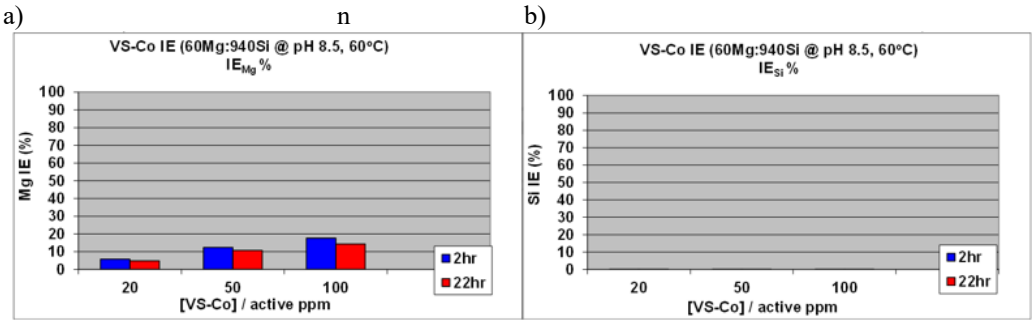

Fig. 7. The inhibition efficiency percentage (IE %) of VS-Co IE was calculated using (a) Mg ion as C_o, IE_{Mg} % and (b) Si ion as C_o, IE_{Si} %

The results were then compared with spectra generated for the commercial samples.

The results show significantly higher silica/silicate scale formation for the blank sample of 60Mg:940Si brine without any VS-Co presence over the samples that were treated with inhibitor. This is because no scale inhibitor is present to stop the scaling ion from reacting to form the silica/silicate scale in the blank solution. All magnesium silicate samples shown in Figure 8 have a similar pattern in terms of peak location

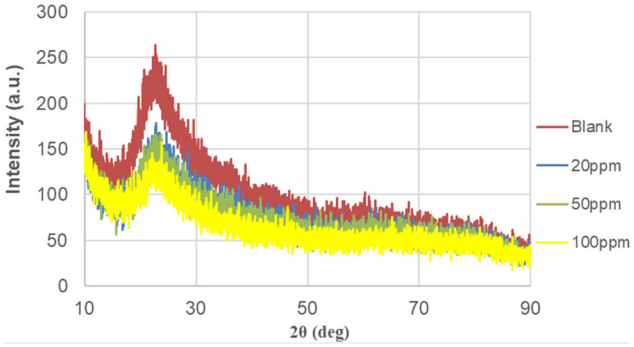

Fig. 8. XRD patterns of the precipitate produced in non-inhibited (blank) and VS-Co inhibited 60Mg:940Si system

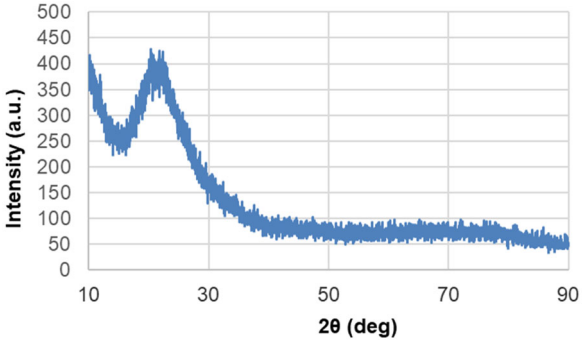

Fig. 9. XRD pattern for commercial amorphous silica, SiO_2

but are different in intensity. The samples exhibited a similar broad peak in the 2θ range from 15-30° corresponding to the XRD of commercial amorphous SiO_2 shown in Figure 9, which is clearly showing amorphous characteristics. Whilst the blank sample of 900Mg:940Si brine in Figure 10 shows a crystalline structure of silica/silicate.

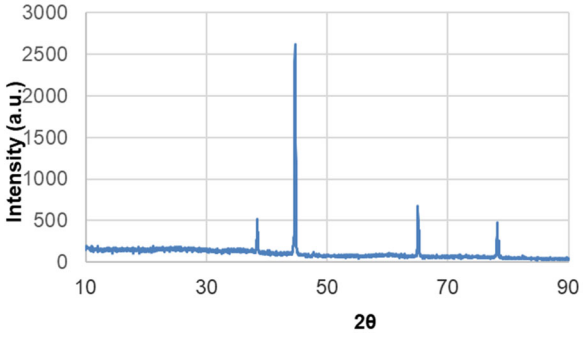

Fig. 10. XRD pattern for non-inhibited 900Mg:940Si system

3.4. Different functional groups identification in precipitates using FTIR

The results of the IR spectra are presented in this section by grouping them into three categories:

1. Blank scaling brine of high Mg^{2+} (900Mg:940Si) in Figure 11;
2. Commercial samples: (a) Magnesium silicate ($MgSiO_3$), (b) Amorphous silica (SiO_2), and (c) Magnesium hydroxide ($Mg(OH_2)$) in Figures 12, 13, and 14, respectively;
3. Blank scaling brine of low Mg^{2+} (60Mg:940Si) in Figure 15;
4. Inhibited scaling brine of low Mg^{2+} with various VS-Co concentrations (60Mg:940Si 20ppm VS-Co), (60Mg:940Si 50 ppm VS-Co), and (60Mg:940Si 100ppm VS-Co) in Figures 16, 17, and 18 respectively.

Three different types of commercial samples, i.e. magnesium silicate, magnesium hydroxide, and amorphous

silica, were analysed using FTIR. These commercial samples were used as a reference to determine the types and morphology of the scale produced in the three systems studied, i.e. the non-inhibited high Mg^{2+} system, the non-inhibited low Mg^{2+} system, and the VS-Co inhibited low Mg^{2+} system.

The spectra for the non-inhibited high Mg^{2+} system in Figure 11 show bands at 1006 cm^{-1} (Si-O covalent band), 780 cm^{-1} (Si-O-Si stretching band), and 670 cm^{-1} are almost identical to the spectra of Figure 12 but at a lower intensity. These confirm the presence of magnesium silicate in the sample. By comparing the IR spectra of this high Mg^{2+} system to the IR spectra of the amorphous silica in Figure 13, it can be seen that the band at ~1000 cm^{-1} is further to the left, i.e. at 1067 cm^{-1}, and the band at ~780 is further to the right, i.e. at ~807 cm^{-1}.

When comparing all the IR spectra with the commercial $Mg(OH)_2$ (Fig. 14), it can be concluded there is no $Mg(OH)_2$ present in the samples which were prepared at pH8.5. This may be because magnesium hydroxide only forms precipitate at ≥ pH 9, and that pH range was avoided in the experiment, hence the absence of $Mg(OH)_2$ [42,43].

Figure 15 shows the IR spectra for the non-inhibited low Mg^{2+} system. It was shown that the band at ~1000 cm^{-1} is almost identical to the peak shown for the commercial amorphous silica, i.e. 1073 cm^{-1}. This low Mg^{2+} system also shows bands at 780 cm^{-1} and 670 cm^{-1}, but they are of lower intensity. Similarly, no peaks were observed to match the one found in the commercial $Mg(OH)_2$; this confirms the pH of this mixed brine was not high enough for magnesium hydroxide to form. From these observations, it can be concluded that most of the Si^{4+} ions were polymerised to form a long chain of the amorphous silica before the Mg^{2+} bridged some of the long-chain SiO_2 backbones. In contrast, in the non-inhibited high Mg^{2+} system, it can be postulated more Mg^{2+} ions bridged the SiO_2 backbone to produce a magnesium silicate scale.

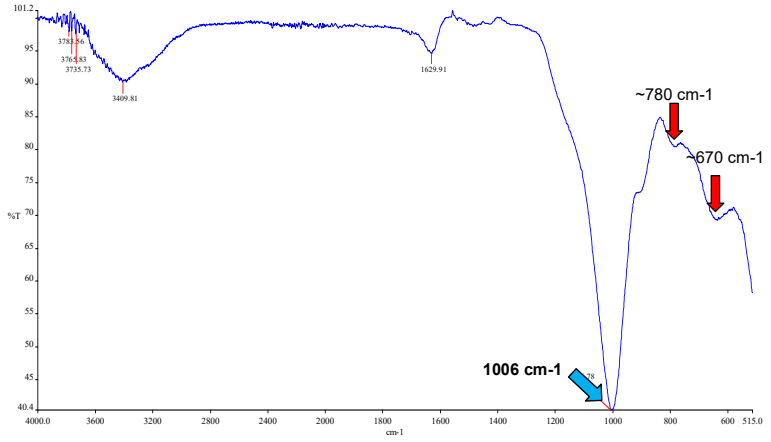

Fig. 11. FTIR spectra for non-inhibited high Mg^{2+} sample system (900Mg:940Si)

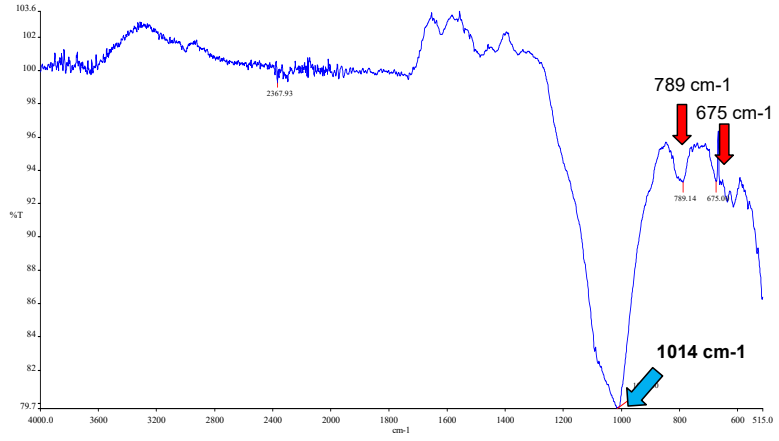

Fig. 12. FTIR spectra for commercial magnesium silicate ($MgSiO_3$)

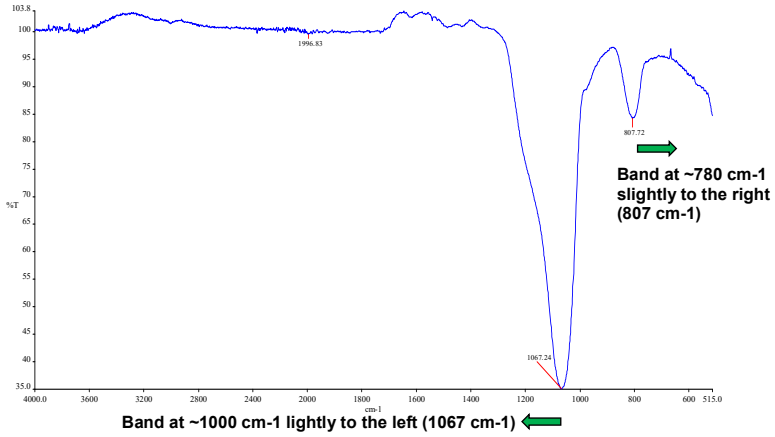

Fig. 13. FTIR spectra for commercial amorphous silica (SiO_2)

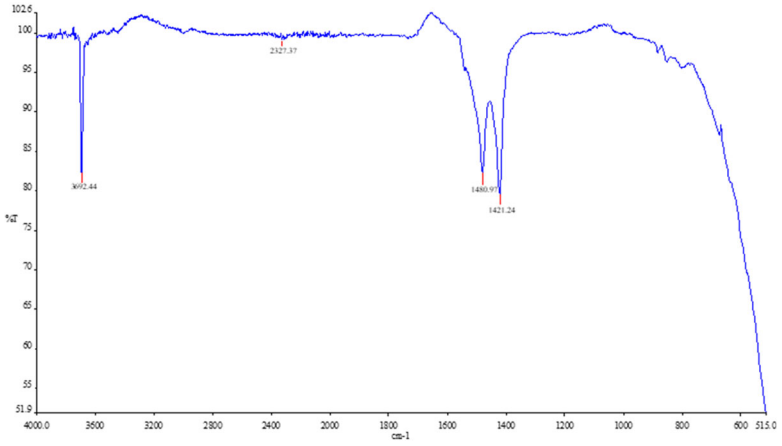

Fig. 14. FTIR spectra for commercial magnesium hydroxide ($Mg(OH_2)$)

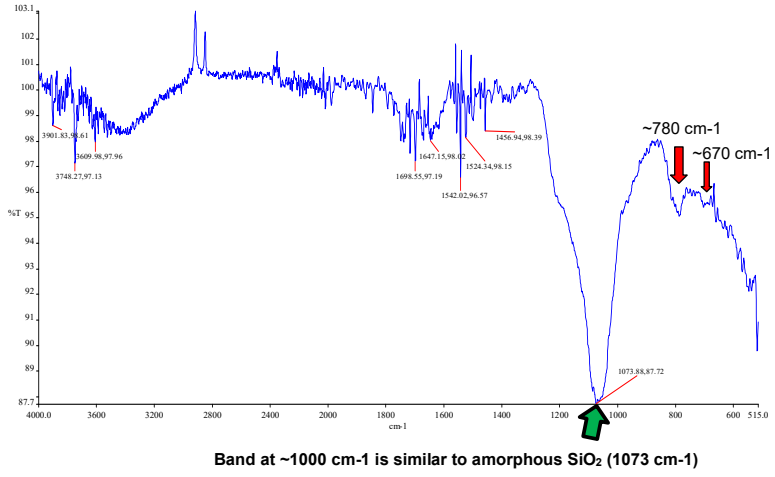

Fig. 15. FTIR spectra for precipitate produced in non-inhibited low Mg^{2+} system (60Mg:940Si)

The IR spectra for the VS-Co inhibited in the low Mg^{2+} system shown in Figure 16 to Figure 18 exhibit a similar band pattern to the blank non-inhibited low Mg^{2+} system in Figure 15. However, the ~1000 cm^{-1} (Si-O covalent band) around 1073 cm^{-1} observed in the non-inhibited scaling brine was moved further to the right when VS-Co was present in the scaling brine. When compared to the band recorded for the high Mg^{2+} system, the Si-O covalent band is nearer to 1000 cm^{-1} (i.e. 1006 cm^{-1}). The bands at ~780 cm^{-1} and ~670 cm^{-1} became less obvious in the VS-Co-inhibited brines, which may explain a lower magnesium silicate scale formed when VS-Co is present. This observation agreed well with the IE_{Mg} % calculated from the ICP-OES analysis in Figure 7, which showed that IE_{Mg} % increased with higher VS-Co concentrations in the scaling brine.

The observed spectra in Figures 16-18 also confirmed that although the sample was inhibited with VS-Co, the silica/silicate scale still formed and resembled an amorphous silica scale (at bands 1058 cm^{-1} to 1070 cm^{-1}) and magnesium silicate (shown in dual-bands at ~780 cm^{-1} and ~670 cm^{-1}). Previous work [44,45] reported peaks for Si-O-Si and Si-O-M (where M=Al, Mg, or Fe) at 950 to 1200 cm^{-1}, whereas other research [46] reported the Si-O stretching vibration shifted from 1111.11 cm^{-1} for pure SiO_2 to 1030.93 cm^{-1} for $MgSiO_3$ and 975.61 cm^{-1} for $Mg_2.4SiO_4$.

Based on these FTIR results and analysis, it can be concluded VS-Co slightly inhibited Mg^{2+} from reacting but completely failed to inhibit the Si^{4+} ions from polymerising and eventually forming an amorphous silica scale, which agreed with the ICP-OES analysis. Nevertheless, the presence of VS-Co in the scaling brine caused an alteration in the frequency of 1400 cm^{-1} to 1600 cm^{-1}. This might happen due to the precipitation of VS-Co with amorphous silica, but further work is required to investigate and prove this observation.

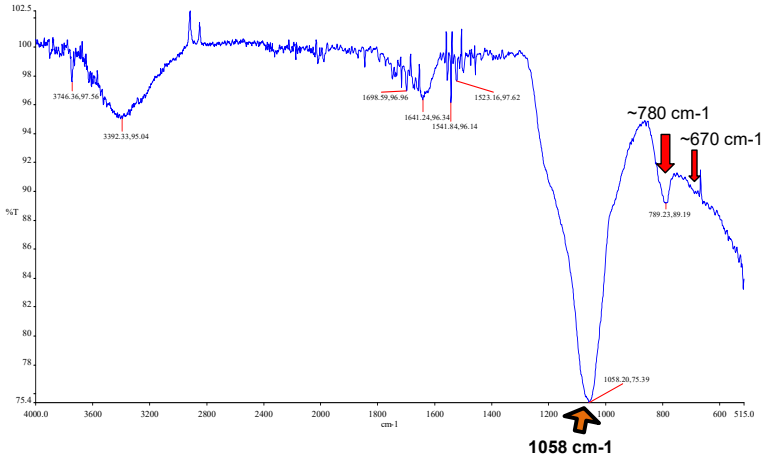

Fig. 16. FTIR spectra for precipitate produced in VS-Co inhibited 60Mg:940Si system (20 ppm VS-Co added)

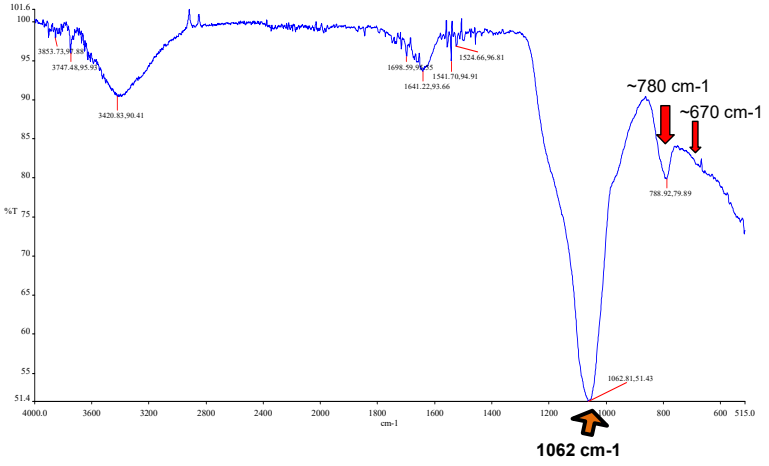

Fig. 17. FTIR spectra for precipitate produced in VS-Co inhibited 60Mg:940Si system (50 ppm VS-Co added)

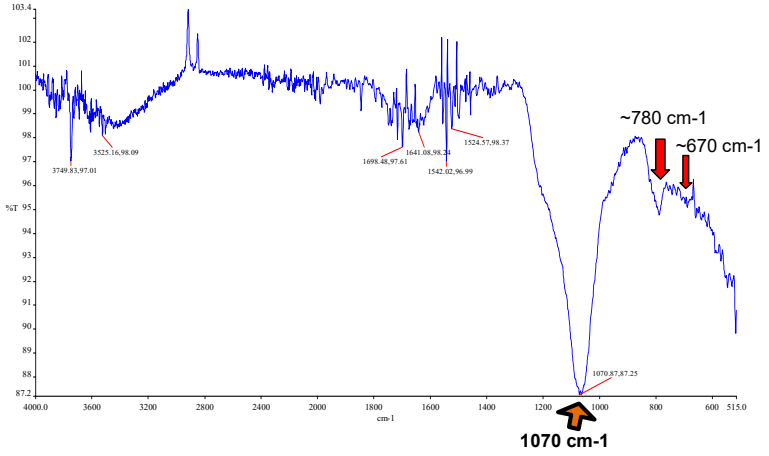

Fig. 18. FTIR spectra for precipitate produced in VS-Co inhibited 60Mg:940Si system (100 ppm VS-Co added)

Similar findings were observed in laboratory work [47], which studied the IE of three SI on calcium carbonate in the presence of EOR chemicals where remarkable ranges of crystal morphologies were detected in precipitates collected.

4. Conclusions

This work studies the effect of vinyl sulfonated copolymer VS-Co as a possible inhibitor/dispersant for the 60Mg:940Si mixed brine system. The X-Ray Diffraction (XRD) results show the inhibited samples with VS-Co at 20 ppm, 50 ppm, and 100 ppm, respectively produce similar structures to the blank non-inhibited sample, showing the amorphous silica was still forming in these VS-Co inhibited samples. This structure was amorphous silica, and hardly any magnesium silicate was generated, which is also supported by the FTIR spectra. However, the sample of 900Mg:940Si shows a crystalline structure with hardly any amorphous silica present, suggesting the sample might remain hydrated for a long period and hence alter the amorphous condition. The IR spectra results also indicate the samples of the 60Mg:940Si brine system have silicate scale formation with low magnesium silicate content when compared to the non-inhibited 900Mg:940Si brine sample.

To conclude, VS-Co could not significantly inhibit silica scale formation even at the highest concentration (100 ppm) of VS-Co. However, having VS-Co present caused an alteration in IR spectra frequency which requires further investigation to assess how best to develop the inhibiting properties of the VS-Co product. Much research on the application of nanoparticles [40, 48-51] might be a head start in new research direction in searching for an efficient method of managing the silica/silicate scale. A modified scale inhibitor with nanosilica (SiO_2–NH_2/PASP) exhibits excellent scale inhibition performance against $CaSO_4$ and $CaCO_3$ at very low concentrations [52]. The modification of potential scale inhibitors with nanoparticles may be able to improve the inhibition efficiency towards the silica/silicate scale.

Acknowledgements

This work is supported by the Ministry of Higher Education (MOHE) Malaysia and Universiti Teknologi MARA (UiTM) under the Fundamental Research Grant Scheme (FRGS/1/2019/TK07/UITM/02/10). Special thanks to the experts and laboratory staff from the Flow Assurance and Scale Team (Heriot-Watt University, United Kingdom) and College of Engineering, Universiti Teknologi MARA (UiTM) for the facilities, help and assistance given to complete this study.

Additional information

Authors to thank the College of Engineering, Universiti Teknologi MARA (UiTM) Shah Alam for the financial aid to present this paper at The 5th International Conference on Engineering Technology 2021 (ICET 2021) was held from October 25th – 26th, 2021 (Fully virtual conference).

References

[1] V.N. Kashpura, V.V. Potapov, Study of the Amorphous Silica Scales Formation At The Mutnovskoe Hydrothermal Field (Russia), Proceedings of the 25th Workshop on Geothermal Reservoir Engineering, Stanford, California, USA, 2000.

[2] H. Guo, Y. Li, F. Wang, Z. Yu, Z. Chen, Y. Wang, X. Gao, ASP Flooding: Theory and Practice Progress in China, Journal of Chemistry 2017 (2017) 8509563. DOI: https://doi.org/10.1155/2017/8509563
[3] Z. Amjad, R.W. Zuhl, An Evaluation of Silica Scale Control Additives, Proceedings of the NACE Corrosion Conference and Expo, New Orleans, USA, 2008.
[4] A.E. Basbar, K.A. Elraies, R.E. Osgouei, Formation Silicate Scale Inhibition during Alkaline Flooding: Static Model, Proceedings of the North Africa Technical Conference and Exhibition, Cairo, Egypt, 2013. DOI: https://doi.org/10.2118/164669-MS
[5] H. Lu, J. Brooks, R. Legan, S. Fritz, Novel Laboratory Test Method and Field Applications for Silica/Silicate and Other Problematic Scale Control, Proceedings of the SPE International Oilfield Scale Conference and Exhibition, Aberdeen, Scotland, UK, 2018. DOI: https://doi.org/10.2118/190705-MS
[6] W. Wang, W. Wei, Silica and Silicate Scale Formation and Control: Scale Modeling, Lab Testing, Scale Characterization, and Field Observation, Proceedings of the SPE International Oilfield Scale Conference and Exhibition, Aberdeen, Scotland, UK, 2016. DOI: https://doi.org/10.2118/179897-MS
[7] J.A. Bush, J. Vanneste, E.M. Gustafson, C.A. Waechter, D. Jassby, C.S. Turchi, T.Y. Cath, Prevention and management of silica scaling in membrane distillation using pH adjustment, Journal of Membrane Science 554 (2018) 366-377. DOI: https://doi.org/10.1016/j.memsci.2018.02.059
[8] J. Arensdorf, D. Hoster, D. McDougall, M. Yuan, Static and Dynamic Testing of Silicate Scale Inhibitors, Proceedings of the International Oil and Gas Conference and Exhibition in China, Beijing, China, 2010. DOI: https://doi.org/10.2118/132212-MS
[9] K.S. Sorbie, N. Laing, How Scale Inhibitors Work: Mechanisms of Selected Barium Sulphate Scale Inhibitors Across a Wide Temperature Range, Proceedings of the 6th SPE International Symposium on Oilfield Scale, Aberdeen, Scotland, UK, 2004. DOI: https://doi.org/10.2118/87470-MS
[10] R.A. Sazali, K.S. Sorbie, L.S. Boak, The Effect of pH on Silicate Scaling, Proceedings of the SPE European Formation Damage Conference and Exhibition, Budapest, Hungary, 2015. DOI: https://doi.org/10.2118/174193-MS
[11] R.A. Sazali, The Development of A Test Methodology and New Findings in Silicate Scale Formation and Inhibition, PhD Thesis, Heriot-Watt University, Edinburgh, United Kingdom, 2018.
[12] G. Ji-jiang, W. Yang, Z. Gui-cai, J. Ping, S. Mingqin, Investigation of Scale Inhibition Mechanisms Based on the Effect of HEDP on Surface Charge of Calcium Carbonate, Tenside Surfactants Detergents 53/1 (2016) 29-36. DOI: https://doi.org/10.3139/113.110407
[13] J. Sonne, S. Kerr, K. Miner, Application of Silicate Scale Inhibitors for ASP Flooded Oilfields: A Novel Approach to Testing and Delivery, Proceedings of the SPE International Conference on Oilfield Scale, Aberdeen, Scotland, UK, 2012. DOI: https://doi.org/10.2118/154332-MS
[14] D.B. van den Heuvel, E. Gunnlaugsson, I. Gunnarsson, T.M. Stawski, C.L. Peacock, L.G. Benning, Understanding Amorphous Silica Scaling Under Well-Constrained Conditions Inside Geothermal Pipelines, Geothermics 76 (2018) 231-241. DOI: https://doi.org/10.1016/j.geothermics.2018.07.006
[15] Y. Qi, T. Tong, X. Liu, Mechanisms of Silica Scale Formation on Organic Macromolecule-Coated Surfaces, ACS ES&T Water 1/8 (2021) 1826-1836. DOI: https://doi.org/10.1021/acsestwater.1c00120
[16] R.A. Sazali, N.S. Ramli, K.S. Sorbie, L.S. Boak, Impacts of Temperature on the Silicate Scale Severity and Morphologies Studies, International Transaction Journal of Engineering, Management, and Applied Sciences and Technologies 12/9 (2021) 12A9R. DOI: https://doi.org/10.14456/ITJEMAST.2021.186
[17] A Fatah, The Effect of Silica Dissolution on Reservoir Properties during Alkaline-Surfactant-Polymer (ASP) Flooding, Journal of Petrochemical Engineering 2/1 (2022) 29-36. DOI: https://doi.org/10.36959/901/251
[18] A.A. Umar, I.M. Saaid, Effects of Temperature on Silicate Scale Inhibition During ASP Flooding, Journal of Applied Sciences 14/15 (2014) 1769-1774. DOI: https://doi.org/10.3923/jas.2014.1769.1774
[19] I. Rashid, N.H. Daraghmeh, M.M. Al Omari, B.Z. Chowdhry, S.A. Leharne, H.A. Hodali, A.A. Badwan, Chapter 7 - Magnesium Silicate, in: H.G. Brittain (ed), Profiles of Drug Substances, Excipients and Related Methodology, vol. 36, Academic Press, Cambridge, MA, 2011, 241-285. DOI: https://doi.org/10.1016/B978-0-12-387667-6.00007-5
[20] J. Arensdorf, S. Kerr, K. Miner, T. Ellis-Toddington, Mitigating Silicate Scale in Production Wells in an Oilfield in Alberta, Proceedings of the SPE International Symposium on Oilfield Chemistry, The Woodlands, Texas, USA, 2011. DOI: https://doi.org/10.2118/141422-MS
[21] U.Z. Husna, K.A. Elraies, J.A.B.M. Shuhili, A.A. Elryes, A review: the utilization potency of biopolymer as an eco-friendly scale inhibitors, Journal of Petroleum Exploration and Production Technology 12 (2022) 1075-1094. DOI: https://doi.org/10.1007/s13202-021-01370-4

[22] D.L. Gallup, Brine pH modification scale control technology. 2. A review, GRC Transactions 35 (2011) 609-614.
[23] D.L. Gallup, pH Modification Scale Control Technology, Proceedings of the International Workshop on Mineral Scaling 2011, Manila, Philippines, 2011, 39-46.
[24] L. Spitzmüller, V. Goldberg, S. Held, J.C. Grimmer, D. Winter, M. Genovese, J. Koschikowski, T. Kohl, Selective silica removal in geothermal fluids: Implications for applications for geothermal power plant operation and mineral extraction, Geothermics 95 (2021) 102141. DOI: https://doi.org/10.1016/j.geothermics.2021.102141
[25] A.D. Dobrzańska-Danikiewicz, Composite materials consisting of carbon nanostructures and nanoforms of selected metals, Archives of Materials Science and Engineering 84/1 (2017) 5-22. DOI: https://doi.org/10.5604/01.3001.0010.3027
[26] K. Szmajnta, M. Szindler, Synthesis and properties of TiO_2, NiO and ZnO nanoparticles and their possible biomedical application, Archives of Materials Science and Engineering 98/2 (2019) 81-84. DOI: https://doi.org/10.5604/01.3001.0013.4612
[27] K. Szmajnta, M.M. Szindler, M. Szindler, Synthesis and magnetic properties of Fe_2O_3 nanoparticles for hyperthermia application, Archives of Materials Science and Engineering 109/2 (2021) 80-85. DOI: https://doi.org/10.5604/01.3001.0015.2627
[28] O.H. Sabr, N.H. Al-Mutairi, A.Y. Layla, Characteristic of low-density polyethylene reinforcement with nano/micro particles of carbon black: a comparative study, Archives of Materials Science and Engineering 110/2 (2021) 49-58. DOI: https://doi.org/10.5604/01.3001.0015.4312
[29] A. Kioka, M. Nakagawa, Theoretical and experimental perspectives in utilizing nanobubbles as inhibitors of corrosion and scale in geothermal power plant, Renewable and Sustainable Energy Reviews 149 (2021) 111373. DOI: https://doi.org/10.1016/j.rser.2021.111373
[30] Lu, H., Liu, Y., Watson, B. (2021) Silicate Scale Inhibitor Evaluation and Applications, Proceedings of the CORROSION 2021, Virtual, 2021.
[31] J. Brooks, H. Lu, M. Barber, Kinetic Turbidity Test Method for Scale Inhibitor Evaluation on Multi-functional Scales, Proceedings of the CORROSION 2021, Virtual, 2021.
[32] M.A. Singleton, J.A. Collins, N. Poynton, H.J. Formston, Developments in PhosphonoMethylated PolyAmine (PMPA) Scale Inhibitor Chemistry for Severe $BaSO_4$ Scaling Conditions, Proceedings of the International Symposium on Oilfield Scale, Aberdeen, Scotland, UK, 2000. DOI: https://doi.org/10.2118/60216-MS
[33] P.H. Gamache, Charged aerosol detection for liquid chromatography and related separation techniques, John Wiley & Sons, Hoboken, 2017. DOI: https://doi.org/10.1002/9781119390725
[34] Z. Amjad, Maleic acid-based copolymers as silica scale control agents for aqueous systems. International Journal of Corrosion and Scale Inhibition 5/1 (2016) 1-11. DOI: https://doi.org/10.17675/2305-6894-2016-5-1-1
[35] Z. Amjad, Silica scale control by non-ionic polymers: The influence of water system impurities, International Journal of Corrosion and Scale Inhibition 5/2 (2016) 100-111. DOI: https://doi.org/10.17675/2305-6894-2016-5-2-1
[36] A. Ünal, Y. Tuğçe Yüksel, Mitigation of Silicate-Stibnite Deposits in Reinjection Wells of Geothermal Power Plants, Biological and Chemical Research 8 (2021) 109-122.
[37] C. Li, C. Zhang, W. Zhang, The inhibition effect mechanisms of four scale inhibitors on the formation and crystal growth of $CaCO_3$ in solution, Scientific Reports 9 (2019) 13366. DOI: https://doi.org/10.1038/s41598-019-50012-7
[38] Z. Amjad, R.W. Zuhl, Silica Control in Industrial Water Systems with a New Polymeric Dispersant, Proceedings of the Association of Water Technologies, Inc. Annual Convention and Exposition, Hollywood, Florida, USA, 2009.
[39] N.P. Chilcott, D.A. Phillips, M.G. Sanders, I.R. Collins, A. Gyani, The Development and Application of an Accurate Assay Technique for Sulphonated Polyacrylate Co-Polymer Oilfield Scale Inhibitors, Proceedings of the International Symposium on Oilfield Scale, Aberdeen, Scotland, UK, 2000. DOI: https://doi.org/10.2118/60194-MS
[40] Benitha, V.S., Monisha, K., Jeyasubramaniyan, K. (2016) Formulation and evaluation of TiO_2.Fe_2O_3 nanopaint, Archives of Materials Science and Engineering 77/1 (2016) 40-44. DOI: https://doi.org/10.5604/18972764.1225546
[41] S.S. Shaw, Investigation into the Mechanisms of Formation and Prevention of Barium Sulphate Oilfield Scale, PhD Thesis, Heriot-Watt University, Edinburgh, United Kingdom, 2012.
[42] S.T. Liu, G.H. Nancollas, The crystallization of magnesium hydroxide, Desalination 12/1 (1973) 75-84. DOI: https://doi.org/10.1016/S0011-9164(00)80176-9

[43] C. Chieng, G.H. Nancollas, The crystallization of magnesium hydroxide, constant composition study, Desalination 42/2 (1982) 209-219. DOI: https://doi.org/10.1016/S0011-9164(00)88753-6
[44] M.A. Karakassides, D. Gournis, D. Petridis, Infrared reflectance study of thermally treated Li- and Cs-montmorillonites, Clays and Clay Minerals 45/5 (1997) 649-658. DOI: https://doi.org/10.1346/CCMN.1997.0450504
[45] M.A. Karakassides, D. Gournis, D. Petridis, An infrared reflectance study of Si-O vibrations in thermally treated alkali-saturated montmorillonites, Clay Minerals 34/3 (1999) 429-438. DOI: https://doi.org/10.1180/000985599546334
[46] C. Jäger, J. Dorschner, H. Mutschke, Th. Posch, Th. Henning, Steps toward interstellar silicate mineralogy VII. Spectral properties and crystallization behaviour of magnesium silicates produced by the sol-gel method, Astronomy and Astrophysics 408/1 (2003) 193-204. DOI: https://doi.org/10.1051/0004-6361:20030916
[47] Q. Wang, F. Liang, W. Al-Nasser, F. Al-Dawood, T. Al-Shafai, H. Al-Badairy, S. Shen, H. Al-Ajwad, Laboratory study on efficiency of three calcium carbonate scale inhibitors in the presence of EOR chemicals, Petroleum 4/4 (2018) 375-384. DOI: https://doi.org/10.1016/j.petlm.2018.03.003
[48] W. Matysiak, T. Tański, W. Smok, Electrospinning of PAN and composite PAN-GO nanofibers, Journal of Achievements in Materials and Manufacturing Engineering 91/1 (2018) 18-26. DOI: https://doi.org/10.5604/01.3001.0012.9653
[49] J. Thanikachalam, P. Nagaraj, S. Karthikeyan, Preparation and characterization of nano magnetic fluid for automotive applications, Archives of Materials Science and Engineering 96/2 (2019) 49-55. DOI: https://doi.org/10.5604/01.3001.0013.2384
[50] W. Matysiak, K. Adamczyk, The analysis of surface morphology, band gaps and optical properties of PAN/GO thin films, Archives of Materials Science and Engineering 101/2 (2020) 49-56. DOI: https://doi.org/10.5604/01.3001.0014.1190
[51] K. Szmajnta, M.M. Szindler, Influence of UV radiation on TiO_2 nanoparticles antibacterial behaviour, Archives of Materials Science and Engineering 101/1 (2020) 25-31. DOI: https://doi.org/10.5604/01.3001.0013.9503
[52] Y. Cheng, X. Guo, X. Zhao, Y. Wu, Z. Cao, Y. Cai, Y. Xu, Nanosilica modified with polyaspartic acid as an industrial circulating water scale inhibitor, npj Clean Water 4 (2021) 46. DOI: https://doi.org/10.1038/s41545-021-00137-y